



ELSEVIER

29 July 1996

PHYSICS LETTERS A

Physics Letters A 218 (1996) 58–63

## The dynamics of sandpiles with a sheared flow

D.E. Newman <sup>a</sup>, B.A. Carreras <sup>a</sup>, P.H. Diamond <sup>b</sup>

<sup>a</sup> Oak Ridge National Laboratory, Oak Ridge, TN 37831-8070, USA

<sup>b</sup> University of California at San Diego, La Jolla, CA 92093-0319, USA

Received 24 April 1996; accepted for publication 26 April 1996

Communicated by M. Porkolab

### Abstract

Sheared wind on a sandpile model produces a decorrelation of transport events and eliminates events with scale lengths on the order of the box size. The effective diffusion coefficient changes its asymptotic behavior from  $D_{\text{eff}} \propto x^\alpha$ , with  $\alpha$  close to 1, to  $D_{\text{eff}} \propto x^0$ . These asymptotic limits are consistent with analytical calculations based on the Burgers equation and have implications for SOC theory as a paradigm for turbulent transport.

Motivated by the complicated dynamics observed in simulations and experiments of gradient driven turbulent transport, a simple paradigmatic transport model based on the ideas of self-organized criticality (SOC) has been developed and investigated [1]. In many cases a strong coupling exists between the turbulence and bulk flows in the system. If the bulk flows are uniform the turbulence imbedded in the flow is simply advected and the dynamics are usually not changed. Often, however, such flows are spatially dependent (sheared) and therefore can have an impact on the dynamics of the system [2,3]. SOC systems have been the focus of much investigation recently due to the broad relevance of many of the characteristics of these systems [4–6]. For example,  $1/f$  noise is a ubiquitous feature in many diverse physical systems from starlight flicker through river flows to stock market data. Additionally many of these systems (and others) exhibit a remarkable spatial and temporal self-similar structure. The physical and dynamical self-similarity that is exhibited by these systems is very robust to perturbations and is not necessarily close to any “linearly marginal”

state such as the angle of repose for a sandpile. It is this self-similarity and non-linear self organization that leads to the term “self-organized criticality” [4]. In many systems (magnetically confined plasmas for example), the transport of constituents down their ambient gradient is thought to be dominated by turbulent transport. That is a turbulent relaxation of the gradient. The turbulence itself is often driven by the free energy in the gradient. It is this combination of turbulent relaxation removing the source of free energy thereby turning off the turbulence which then allows the gradient to build back up which allows the development of robust (albeit fluctuating) profiles. The dynamics of such systems can be computationally investigated with a cellular automata model of a running sandpile. This model allows us to investigate the major dynamical scales and the effect of an applied sheared flow on these dominant scales. In addition to allowing the paradigmatic investigation of turbulent transport, the introduction of sheared flow (wind) and the determination of transport coefficients in sandpiles, both of which naturally arise in the context of magnetically confined plasmas, act as

a novel and important extension to the chaotic dynamics of SOC systems.

Starting from the assumptions of the importance of near marginality to turbulent transport and the importance of turbulent transport to relaxation of gradients a very simple natural model presents itself. The relationship between the simple “sandpile” model and turbulent transport can best be summarized as follows. In this model local turbulent fluctuations are excited by the local gradient exceeding marginality, the local fluctuations in turn relax the local gradient, transporting the excess gradient down the profile. This sandpile SOC model has the gradient modeled by the slope of the sandpile while the turbulent transport is modeled by the local amount which falls, overturns, when the sandpile becomes locally unstable. The system is driven by noise from the sources of the transporting quantities or fluctuations in the background transport which in the sandpile model is represented by a random “rain” of sand grains on the pile. This model allows us to study a paradigm of the dynamics of the transport independent of the local instability mechanism and independent of the local transport mechanism.

A standard cellular automata algorithm [7] is used to study the dynamics of the driven sandpile. The domain is divided into cells which are evolved in steps. First, sand grains are added to the cells with a probability  $P_0$ . Next, all the cells are checked for stability against a simple stability rule and either flagged as stable or not and finally the cells are time advanced, with the unstable cells overturning and moving their excess “grains” to another cell with the size, distance and direction of the fall being determined by the overturning rule. The most simple set of rules used are: if  $Z_n \geq Z_{\text{crit}}$  then  $h_n = h_n - N_f$  and  $h_{n+1} = h_{n+1} + N_f$ . With  $h_n$  defined as the height of cell  $n$ ,  $Z_n$  being the difference between  $h_n$  and  $h_{n+1}$ ,  $Z_{\text{crit}}$  is the critical gradient and  $N_f$  is the amount of sand that falls in an overturning event. In terms of the normal physical quantities we associate with turbulent systems,  $Z_{\text{crit}}$  is the critical gradient at which fluctuations are unstable and grow while  $N_f$  is the amount of gradient that is transported (or relaxed) by a local fluctuation.

The simulations are done in a two-dimensional system where  $x$  is equivalent to the radial coordinate (down the sandpile) and  $y$  to the poloidal angle

(around the sandpile), the sandpile is periodic in this direction. We have used a variety of domain sizes varying from 50 by 1 ( $x$  and  $y$  directions) to 800 by 100 with most of the 2D calculations being performed at 200 by 50. The boundary conditions for the computation domain are periodic in the  $y$  direction, open at  $x = L$  (particles that reach the edge are lost) and closed at  $x = 0$ . Computations are typically started from a marginal state (i.e.  $Z_n = Z_{\text{crit}} - 1$ ) and allowed to relax to the steady state. In order to accumulate sufficient statistics the system is iterated for  $10^5$  to  $10^7$  time steps after saturation is reached. The main diagnostic for the sandpile model avalanche dynamics is the time history of the number of flips (overturning events), with both the total number in the system and the number for flips for individual  $y$  values tracked.

One of the characteristics of a SOC system is that steady state time average profiles are globally linearly stable (sub-marginal) and yet are able to maintain active transport dynamics. This is in contrast to naive marginal stability arguments. The one condition needed for the maintenance of a sub-critical profile rather than a marginal profile is that  $N_f$  be greater than 1. This is equivalent to saying that a turbulent eddy will attempt to transport enough to level the local gradient in one eddy turnover. If  $N_f = 1$  then whenever a sand grain is dropped onto the pile it will fall all the way down to the bottom of the pile and exit at the base. This fall is not an organized avalanche in the sense that it will not grow as cascades down the pile because only the local cell with the extra grain is unstable (super-marginal).

For the transport problem, an important parameter to introduce is the effective diffusivity in the steady state,  $D_{\text{eff}}$ .  $D_{\text{eff}}$  is defined as the ratio of the averaged local flux to the averaged local gradient,  $D_{\text{eff}} = \langle \Gamma \rangle / |\langle dh/dx \rangle|$ . Since the system is in steady state, the average local flux through a radial position  $x_0$  is simply the average number of grains falling into the region above  $x_0$ , that is  $P_0 x_0$ . Therefore,  $D_{\text{eff}} = P_0 x_0 / |\langle dh/dx \rangle|$ . The general dependence of  $\langle dh/dx \rangle$  on  $N_f$  can be determined by calculations in which  $P_0$  is held constant and  $N_f$  is varied. It is found that the dependence of  $\langle dh/dx \rangle$  on  $N_f$  is linear, in particular for  $Z_{\text{crit}} = 80$ ,  $\langle dh/dx \rangle \approx 80 - 0.5N_f$ . Keeping in mind that  $N_f$  is the amount that falls, or how much the gradient is relaxed, when a

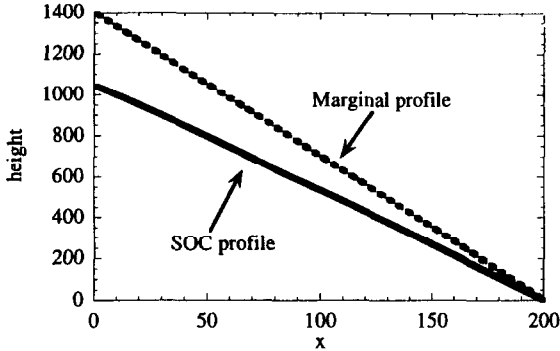


Fig. 1. The time average steady state profiles of a marginal sandpile ( $N_f = 1$ ) and a SOC sandpile ( $N_f = 3$ ) with all other parameters the same. Since both have the same grain drop rate they are therefore transporting the same flux.

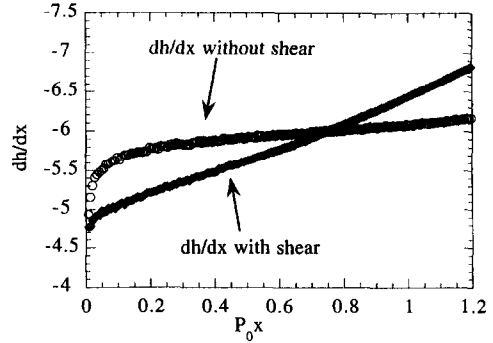


Fig. 2. The slope of the sandpile as a function of  $P_0 x$  for cases with and without shear for  $N_f = 3$ ,  $Z_{crit} = 8$ ,  $P_0 = 0.007$  and  $L = 200$ . Note the change in functional form and the region with  $P_0 x > 0.7$  in which the slope is greater than the shear free SOC slope.

site becomes unstable this dependence indicates how sub-marginal on average a system is likely to be given a local transport mechanism. Additionally the numerical calculations indicate that, for a fixed value of  $N_f$ ,  $\langle dh/dx \rangle$  is essentially a function of  $P_0 x$ . For a fixed  $N_f$ , the numerical results for several values of  $P_0$  and different box sizes collapse in a single curve when plotted versus  $P_0 x$  (Fig. 2). This function is well described by a function of the form

$-\lambda(P_0 x)^\epsilon$ . The coefficient  $\lambda$  is a linear function of  $N_f$ , the exponent  $\epsilon$  has a weaker dependence on  $N_f$ , for  $N_f = 3$ ,  $\epsilon = 0.02 \pm 0.01$ . Hence,  $D_{eff}$  has a functional dependence of  $(P_0 x)^\beta$  with  $\beta = 1 - \epsilon \approx 0.98$ . This result is consistent with the analytical determinations [2,4] of the diffusion coefficient. These calculations are limited to the range  $P_0 x < N_f/2$ . When the average local flux exceeds  $N_f/2$  a distinct change

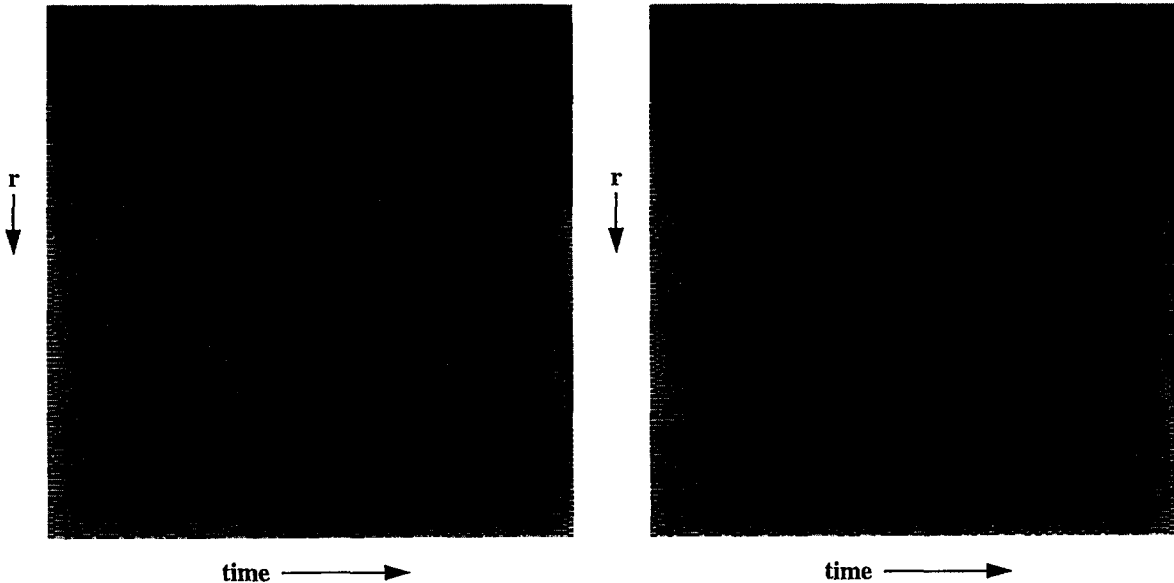


Fig. 3. Time histories of the avalanches at a fixed  $y$  both with and without sheared flow in the middle. The case without the flow shows avalanches of all lengths stretching across the entire domain while the case with sheared flow exhibits a breakup of the avalanches in the sheared region (the center).

in the dynamics occurs. The average local gradient jumps from the sub-marginal SOC gradient to a super-marginal gradient. This jump is coincident with a region in which the avalanches are occurring almost constantly as would be implied by the super-marginal gradient. This region allows for a natural definition of an edge zone, but precludes the extension of the scaling calculations to large values of  $P_0 x$ .

Into the basic model described above we can also add a shear flow in the  $y$  direction (sheared wind blowing on the sandpile). This is implemented by adding a constant flow in one direction to the top of the sandpile and a constant flow in the other direction to the bottom. The two constant flow regions are then connected by a linear shear flow region. The shear is defined as the velocity increment,  $\Delta V$ , between two adjacent cells in the  $x$  direction. The flow is added to the dynamics in the time advance step after moving any falling grains to their new positions. The impact of the shear flow is quantified by changing a shear parameter,  $S$ , equal to  $\Delta V$  times the size of the shear region,  $L_S$  ( $S = L_S \Delta V$ ).

The effect of the shear flow on the transport dynamics can be first and most easily observed in a time history of the overturning sites in the sandpile (Fig. 3). The sheared region in the middle of the domain is easily differentiated from the unsheared ends by the absence of correlated transport events (avalanches) in the shear zone. The difference in avalanche dynamics is visually striking and shows

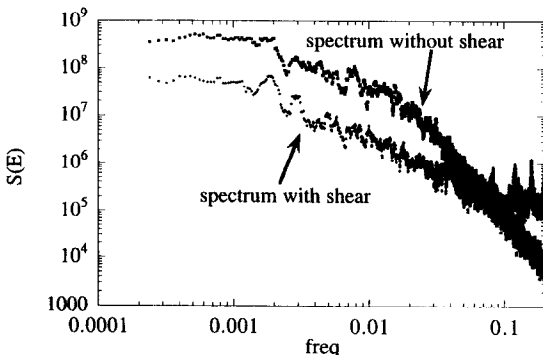


Fig. 4. Frequency power spectra of the number of flips for a simulation with shear and one without shear. Note the decrease in power at low frequency and the increase in power at high frequency.

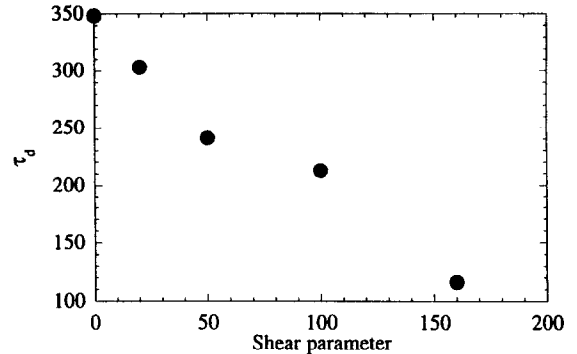


Fig. 5. The decorrelation time  $\tau_d = 1 / [\int \omega S(E) d\omega / \int S(E) d\omega]$  as a function of the shear parameter. Note that the decorrelation time decreases with increasing shear parameter suggesting fewer long transport events and more short ones.

clearly the decorrelation of transport events by the shear flow. In the PDF of the flips, one can see a marked decrease in the variance for a running sandpile with shear when compared to one without shear. This trend continues when the shear and size of the shear zone increase. This suggests that the larger scale transport events are being suppressed by the shear and, since the total flux must remain the same, the medium and small scale events must increase to make up the difference. It should be kept in mind that the number of flips is not strictly a measure of avalanche size as 3 avalanches of size 5 occurring at the same time give the same number of flips as one avalanche of size 15. Therefore the decorrelation of the large scale avalanches must be made up to some degree by multiple simultaneous small slides. Comparing the frequency spectra of the number of flips for an unsheared case with a sheared case (Fig. 4) one can see a suppression of the low frequency end of the spectrum and an increase in the high frequency end. This effect can be quantified through the mean frequency  $\bar{\omega}$ ,  $\bar{\omega} = \int \omega S(E) d\omega / \int S(E) d\omega$ . Fig. 5 shows the variation in  $\tau_d = 1 / \bar{\omega}$  as the shear parameter is increased. This figure shows the decorrelation time of the transport decreasing as the shear parameter increases. Because it is transport events which are being modified and not the underlying fluctuations this transport decorrelation time should not be identified with the standard turbulent decorrelation time. In the shear free case the transport decorrelation time is longer than  $L^2$  while in the

sheared case the decorrelation time becomes shorter than  $L^2$ .

In the shear flow region, there is a substantial change of the steady state sandpile slope. Again we find a universal curve for  $\langle dh/dx \rangle$  when plotted versus  $P_0 x$  (Fig. 2). In this case, the slope of  $h$  cannot be described by a power function, but is just a linear function of  $P_0 x$ . As a consequence, the effective diffusion coefficient is

$$D_{\text{eff}} = \frac{P_0 x}{a + bP_0 x}. \quad (1)$$

Asymptotically, for  $x \rightarrow \infty$ ,  $D_{\text{eff}} \rightarrow b^{-1}$  and becomes independent of  $x$ . For  $N_f = 3$  and  $\Delta V = 1$ , a fit to all the data gives  $a = 4.85$  and  $b = 1.59$ . This change in functional form is consistent with the change in dynamics predicted by analytic work on the Burgers equation model by Diamond and Hahm [1]. The analytic form of the diffusion coefficient goes from infrared divergent ( $D \propto k_r^{-1}$ ) in the shear free case to independent of  $k_r$  ( $D \propto k_r^0$ ) in the sheared flow case. The asymptotic limit ( $x \rightarrow \infty$ ) of the diffusion coefficients in the sandpile model shows the same dependence going to a constant with shear and  $k_r^{-0.98}$  without.

Due to the discrete nature of the system the impact of increasing  $\Delta V$  saturates when  $\Delta V$  is larger than one. This is because when  $\Delta V$  is larger than one all avalanches down to the cell size are decorrelated. Strong sheared flow with a given scale length will decorrelate all transport events with a larger scale length. Therefore, if the shear scale length is made smaller than the smallest transport event (which would be unphysical in a continuous turbulent system) all the avalanches would be decorrelated. Because of this effect, the method used to investigate the dependence of the asymptotic  $D_{\text{eff}}$  on the shear rate was to decrease  $\Delta V$  below 1. The effective asymptotic diffusivity is found to decrease with increasing shear as  $D_{\text{eff}} \propto (\Delta V)^{-0.51}$ . This is in comparison to the analytic form from the Burgers equation which gives a  $D_{\text{eff}}$  dependence on  $\Delta V$  with  $\gamma = 4/5$ . While the coefficients are not the same, given the differences in the models, one being continuous the other being discrete, the qualitative agreement is remarkable.

To compare analytical and numerical functional

dependences on  $P_0$  is not easy. The reason is that to determine this dependence it is necessary to go to relatively large values  $P_0$ , but due to the restriction  $P_0 x < N_f/2$ , this implies  $x \rightarrow 0$ . In this limit, the separate dependence of  $D_{\text{eff}}$  on  $P_0$  is very weak.

In the model as presented up to this point, the inclusion of shear either can cause a transport barrier (for  $P_0 x > N_f/4$ ), a steepening of the gradient with the coincident decrease in the effective diffusion coefficient, or an anti-transport barrier (for  $P_0 x < N_f/4$ ) in which the gradient is further reduced and the effective diffusion coefficient is therefore increased. The first region is the regime relevant to systems in the continuous limit. Additionally, it should be kept in mind that the modification of the critical slope (linear stabilization) by the shear flow effect has not been included in this model.

In conclusion, within the constraints of a cellular automata model of critical gradient dynamics (the running sandpile model) it is found that:

(1) The addition of sheared flow to the running sandpile has a major impact on the transport dynamics. The dominant transport events move from system size to smaller scales.

(2) With moderately strong driving the inclusion of shear can cause the formation of a “transport barrier” (a region with decreased diffusivity). However in this model, which does not include shear effects on linear stability, very weak driving can lead to an increased diffusivity in the shear region. When  $Z_{\text{crit}}$  is modified to include shear stabilization in an ad hoc manner the shear region always exhibits a decreased diffusivity with the coincident transport barrier.

The use of a SOC model as a paradigm for turbulent transport shows much promise in the model ability to capture many aspects of the dynamics independent of the details of the local turbulence drive. Some of these features include:

(a) Robust transport can occur with profiles which are on average sub-marginal. This may be relevant to the experimental observations in magnetically confined plasmas that over much of the radius the profile appears to be marginal or sub-marginal to most of the modes suspected of dominating transport.

(b) Transport events, avalanches, are found on all size and time scales in the running system. The

coherence of large transport events can make the transport scale with the system size even though the local transport mechanism is much smaller scale.

(c) A distinct transition in the scaling of transport dynamics is observed with the addition of a sheared flow. This type of behavior is observed to occur in turbulent systems and may be related to the L–H transitions in magnetically confined plasmas [8].

Valuable discussions with T.S. Hahm and J.-N. Leboeuf are gratefully acknowledged. D.E. Newman would like to thank Oak Ridge National Laboratory for its support through the Wigner Fellowship program. This work is sponsored by Oak Ridge National Laboratory, managed by Lockheed Martin Energy Research Corp. for the U.S. Department of Energy under contract number DE-AC05-96OR22464, and Grant No. De-FG03-88ER-53275.

## References

- [1] P.H. Diamond and T.S. Hahm, On the dynamics of turbulent transport near marginal stability, *Phys. Plasmas*, in press.
- [2] L. Sirovich, ed., *New perspective in turbulence* (Springer, Berlin, 1991).
- [3] H. Biglari, P.H. Diamond and P.W. Terry, *Phys. Fluids B* 2 (1990) 1.
- [4] P. Bak, C. Tang and K. Wiesenfeld, *Phys. Rev. Lett.* 59 (1987) 381.
- [5] T. Hwa and M. Kardar, *Phys. Rev A* 45 (1992) 7002.
- [6] J.M. Carlson and J.S. Langer, *Phys. Rev. Lett.* 62 (1989) 2632.
- [7] L.P. Kadanoff, S.R. Nagel, L. Wu and S-M. Zhou, *Phys. Rev. A* 39 (1989) 6524.
- [8] T.C. Luce et al., in: *Proc. Fifteenth Int. Conf. on Plasma physics and controlled fusion research*, Paper A-2-111-2, Seville, Spain (1994).